Proceedings World Geothermal Congress 2020+1
Reykjavik, Iceland, April - October 2021

Simulation of Seismic Imaging of Supercritical Geothermal Reservoir Using the Full-Waveform Inversion Method

Junzo Kasahara[1,3], Yoko Hasada[2], and Haruyasu Kuzume[1]

[1]ENAA, Toranomon Marine Building 10th, 3-18-19, Toranomon, Minato, Tokyo, Japan

[2] Daiwa Exploration and Consulting Co. Ltd., 5-10-4 Toyo, Koto, Tokyo, Japan

[3]Shizuoka University, Center for Integrated Research and Education of Natural Hazard, 836 Ohya, Shizuoka, Japan

kasahara.junzo@shizuoka.ac.jp

Keywords: Supercritical water, geothermal energy, full-waveform inversion, time lapse, DAS, physical properties, active seismic source, passive seismic source

ABSTRACT

To investigate the imaging capability for supercritical water reservoir as one of the future geothermal energy sources, we performed simulations using the full-waveform inversion (FWI) method. We studied three cases: one using buried active source(s), one involving a more realistic case that considered the Medipolis geothermal field, and one using nearby natural earthquakes as passive seismic sources. In the first case, we assumed a borehole active seismic source at a depth of 2 km combined with seismic arrays at the surface and in the borehole, observation well, and horizontal well. The distributed acoustic sensor (DAS) was used as an array sensor in the borehole, which provided extremely dense seismic data. The FWI result showed very precise location, shape, and physical properties (Vp, Vs, and density) of the reservoir model. In the second case, almost all of the location and shape of the assumed reservoir were retrieved, but the physical properties were not well retrieved. The cause of these results was probably due to the aperture coverage of the observed system. In the third case, we examined the occurrence of nearby natural earthquakes. This case demonstrated reasonable location and shape of an igneous intrusion. However, the physical properties inside the intrusive body were not well retrieved, probably due to the limited locations of the assumed natural earthquakes. In a future field study, we will use both active and passive sources to obtain better imaging of supercritical water reservoirs. We believe that a supercritical water zone can be well imaged using the combination of the FWI method, active seismic sources, adequate natural earthquake data, DAS seismic array(s) in the borehole, and ground surface seismic array. However, retrieval of the physical properties of reservoir(s) can be controlled by the aperture of a seismic observation array.

1. INTRODUCTION

Supercritical water has attracted the attention of the world geothermal community as important future renewable energy. In the Kakkonda geothermal field, scientific drilling of the WD-1a geothermal well revealed that the temperature was higher than 500 °C at a depth of 3,800 m, and the water was believed to be in a supercritical state (Muraka *et al*., 1998). IDDP-1 (Dobson *et al.*, 2017; Reinsch *et al.*, 2017) and IDDP-2 (Friðleifsson *et al*., 2017) in Iceland and Larderello in Italy (Bertani *et al.*, 2018) are some other examples. Because of the increase in the energy consumption in Japan, geothermal energy has become one of the most important energy sources. In Japan, the New Energy and Industrial Technology Development Organization (NEDO) is promoting the development of supercritical geothermal sources for future energy source. As part of the NEDO supercritical project, we examined the possibility of using supercritical water as an alternative new energy source (Kasahara *et al*., 2018b, Suzuki *et al.*, 2018). In particular, we focus on determining the location, thickness, and shape of supercritical water reservoirs and their physical properties such as Vp, Vs, and density.

In our approach, we plan to use active and/or passive seismic sources, distributed acoustic sensor (DAS) technology for receivers, and the full-waveform inversion (FWI) method for data analysis (Kasahara *et al*., 2018a). For imaging of oil and gas, we have used the backpropagation method such as the time-reversal method (Kasahara and Hasada, 2016) in which a receiver array acts as pseudo-seismic sources. The optical fiber in the DAS system can sense acoustic vibrations caused by seismic waves (Hartog, 2017). Because the DAS system provides seismic data at every few meters along the optical-fiber length, DAS can provide dense pseudo-seismic sources for imaging of supercritical water reservoirs. In 2017, we evaluated the usefulness of the DAS method for geothermal purposes and found that the sensitivity was slightly lower than that of ordinary seismometers. However, the system could provide an extremely dense seismic array with a sensor interval that was as short as a few meters (Kasahara *et al*., 2018a, Hasada *et al*., 2018). The optical fiber can be used up to 500 °C, but even geophones in a dual flask cannot be used in such high-temperature conditions for days.

Learning the physical properties and migration with time of supercritical reservoir(s) are very important to retrieve heat from these extremely hot reservoirs. We propose to employ the seismic time-lapse technology to learn the physical properties of supercritical water zones as well as their location, thickness, and shape and to monitor their temporal change. In the seismic-reflection survey, the seismic-migration method is frequently used. Recently, the FWI method has been applied for subsurface imaging. The FWI method used in this study is similar to the time-reversal or backpropagation technique based on the reciprocal principle of Green's function. In the seismic-reflection imaging, the FWI method, not the time-lapse method, has been applied to 3D seismic data. To estimate the physical properties at the target zone, we apply the FWI method to investigate supercritical water. Many FWI studies have been conducted (Tarantola, 1984, 1986; Virieux and Operto, 2009; Tromp *et al*., 2005; Alkalifah, 2016; Schuster, 2017). In our current FWI study, we use the adjoint method developed by Tromp *et al.* (2005) to image supercritical reservoirs and retrieve the change in their physical properties. In this method, the sensitivity kernels for bulk modulus, rigidity, and density can be

obtained using the adjoint method through backpropagation and cross-correlation. By using these sensitivity kernels of elastic constants and density, we can calculate the sensitivity kernels of Vp, and Vs for the inversion process. In our FWI simulations, we use the active and passive seismic sources and DAS system in the borehole as well as the ground surface seismometer array.

In 2018 November, we carried out a feasibility study in the Medipolis geothermal field located in the southern part of Kyushu Island, Japan (Kasahara *et al*., 2019a). During this period, we observed distinct waveforms of natural earthquakes on the surface geophones. The vertical component showed the first P arrivals, and the horizontal components showed large arrivals at approximately less than 1 s later although the vertical component did not show such arrivals. The general explanation of such characteristics could be the P-to-S conversion that occurred at the interface between a soft sedimentary layer and a basement rock layer. Kasahara *et al.* (2019b) interpreted the waveforms observed at the Medipolis geothermal field as a P-to-S conversion at a depth of 4 km beneath the test field. In the present study, we evaluated the possibility of detecting reservoirs that possibly caused such P-to-S conversion using the active seismic source method with FWI.

2. FWI MODELS

In the present study paper, we examine three FWI cases. FWI model-1 represents a case of active seismic source located in the downhole at a depth of 2 km (Figure 1; 3-km-distance source location). We assume a buried seismic source at a depth of 2 km. We examine three source locations and reconstruct the image. We use a 1-km long × 200-m thick supercritical reservoir at a depth of 4 km. We assume the following physical property changes: $\Delta Vp = -5\%$, $\Delta Vs = -5\%$, and $\Delta\rho = -2\%$. For the borehole seismic receivers, we use an optical-fiber DAS system. We employ one of the DAS technologists to provide the strain rate at 1-kHz sampling (Hartog, 2017).

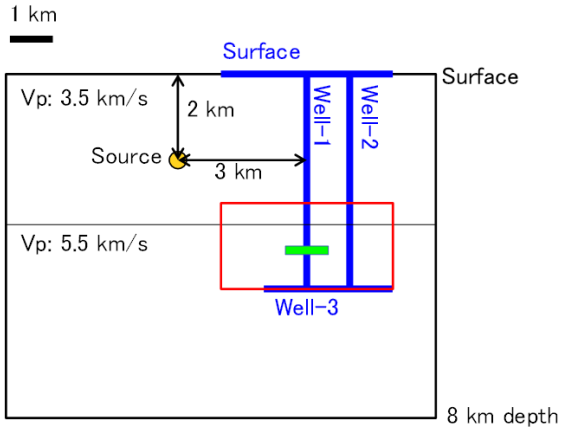

Figure 1: FWI model-1. (Green rectangle) A rectangular (1-km wide and 0.2-km high) supercritical water reservoir is assumed at a depth of 4 km. (Yellow circle) A buried seismic source 3 km from the drilling borehole (Well-1) is examined. Three DAS systems are considered, namely, the drilling borehole (Well-1), observation borehole (Well-2), and horizontal borehole (Well-3), beneath the assumed reservoir. (Blue line annotated as surface) A ground surface geophone array is also used (the red rectangle shows the area used in the FWI).

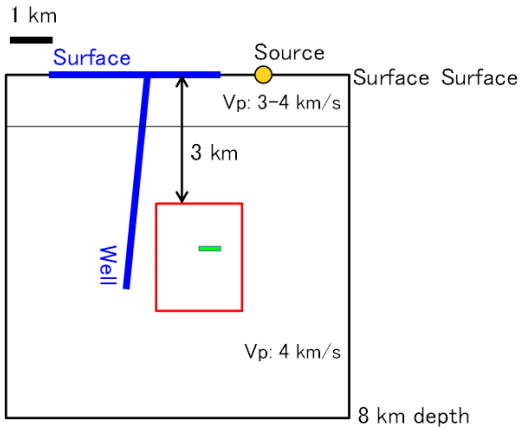

Figure 2: FWI model-2. Evaluation of the field study on whether a 4-km deep reservoir can detect a P-to-S conversion or not. (Green rectangle) A 500-m long and 100-m thick rectangular reservoir is located at a depth of 4 km. No density change is assumed. (Yellow circle) A vertical single force is applied at 6-km distance from the left edge of the model. Vp/Vs = 3 in the assumed reservoir. The red rectangle shows the area used in FWI.

FWI model-2 is a more realistic case, which reflects the Medipolis geographical conditions. We use a vertical single force applied at 6-km distance from the left side. A 500-m long and 100-m thick reservoir is assumed at a depth of 4 km. By using the P-to-S conversion arrivals observed in the 2018 Medipolis experiment, we estimate the Vp/Vs of the reservoir (Kasahara *et al*., 2019b).

The forward simulation shows that the amplitude ratio of the first P arrival versus the P-to-S conversion phase is explained by Vp/Vs = 3 (Kasahara *et al.*, 2019b). In FWI model-2, Vp/Vs = 3 in the reservoir is assumed. DAS in the borehole and surface geophone array are assumed to be installed in the Medipolis geothermal field. However, we consider the horizontal components using DAS because a helical fiber will be introduced in the future.

In FWI model-3, we examine the application of nine natural earthquakes as seismic passive sources surrounding an igneous intrusion, although this is also an idealistic case (Figure 3). In this case, the top of the igneous intrusion is located at a depth of 4 km.

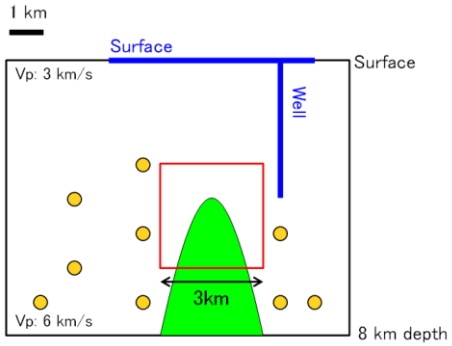

Figure 3: FWI model-3. (Yellow circles) Nine natural earthquakes surrounding (green area) an igneous intrusion. (Blue lines) Ground surface geophone array and a DAS in the borehole at a depth of 4 km are used in FWI. The red rectangle shows the area used in FWI.

3. RESULTS OF THE FWI SIMULATIONS

3.1 Results in the case of buried active source in FWI model-1

The study model is shown in Figure 1. Figure 4 shows examples of the waveforms obtained by all receiving points in Figure 4. The top of the figure shows the surface seismometers, DAS systems in the two vertical wells (well-1 and well-2), and horizontal borehole (well-3). The residual waveforms before and after the change in the physical property change are shown at the bottom in Figure 4. The waveform changes at the surface seismometer array are small, which suggest that the contribution of this array is less significant for imaging. When we examine the usefulness of the horizontal borehole, we recognize that it is highly effective for this inversion.

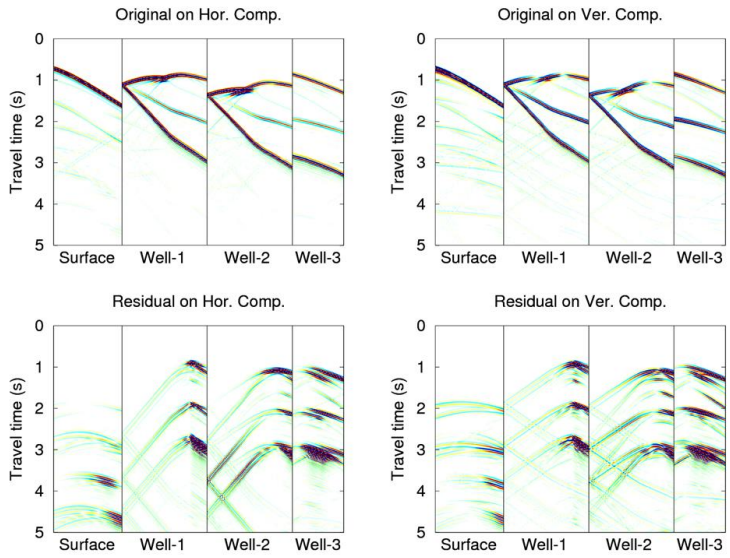

Figure 4: (Top) (left) horizontal and (right) vertical component waveforms of the geophones at the surface, DAS in the borehole (well-1), DAS in the observed borehole (well-2), and DAS in the horizontal borehole (well-3) in each diagram. (Bottom) Residual waveforms of the horizontal and vertical components before and after the change. The vertical axis in each diagram shows the travel time in seconds. The source location is at 3-km distance from the drilling well (see Figure 1).

Although three sources, which are located at 1, 3, and 5 km from the drilling borehole, are evaluated, the case at the 3-km distance shown in Figure 5 exhibits the best results among the three cases. The assumed rectangular shape of the reservoir is almost retrieved. After several iterations by FWI, the Vp, Vs, and density values are retrieved as 4%, 4%, and 2%, respectively, with

almost exact location, thickness, and satisfactory physical property values. However, FWI model-1 is too idealistic because the seismic sources are buried at a depth of 2 km and one horizontal and two vertical wells are used in the inversion.

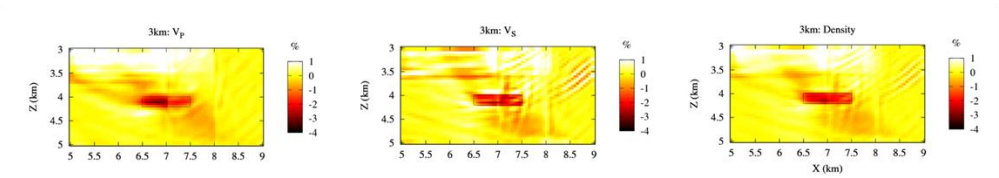

Figure 5: Simulation result of FWI model-1 for the source location at 3-km distance from the drilling borehole. Left to right: Vp, Vs, and density.

3. 2 Results of FWI for Model-2

We examine the usefulness of our seismic study for realistic seismic source(s) and seismic receivers, as presented in FWI model-2. Using FWI model-2, we generate synthetic waveforms, as shown in Figure 6. Intense PS and SS reflections appear on the horizontal component at the right-hand side of the surface geophones. PP and PS reflections appear in the vertical component of the surface geophones. On the other hand, PS and SS are observed in the shallow part of the horizontal component. DAS in the deeper part exhibits PP and PS reflections.

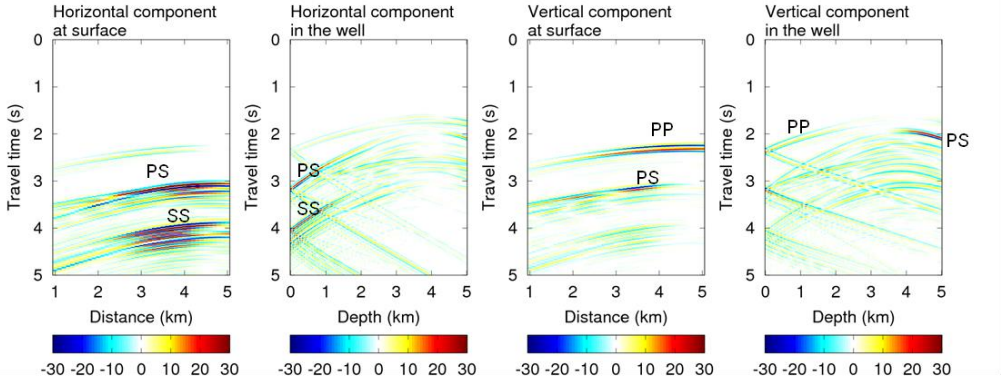

Figure 6: Residual waveforms between the uniform initial model and true model of FWI model-2. Relatively small P and large PS phases are observed in the horizontal components. Vp/Vs = 3 in the reservoir, which is obtained by forward modeling to generate the P-to-S conversion. PP, PS, and SS phases are observed in the reservoir. PP, PS, SS are reflected phase at the reservoir.

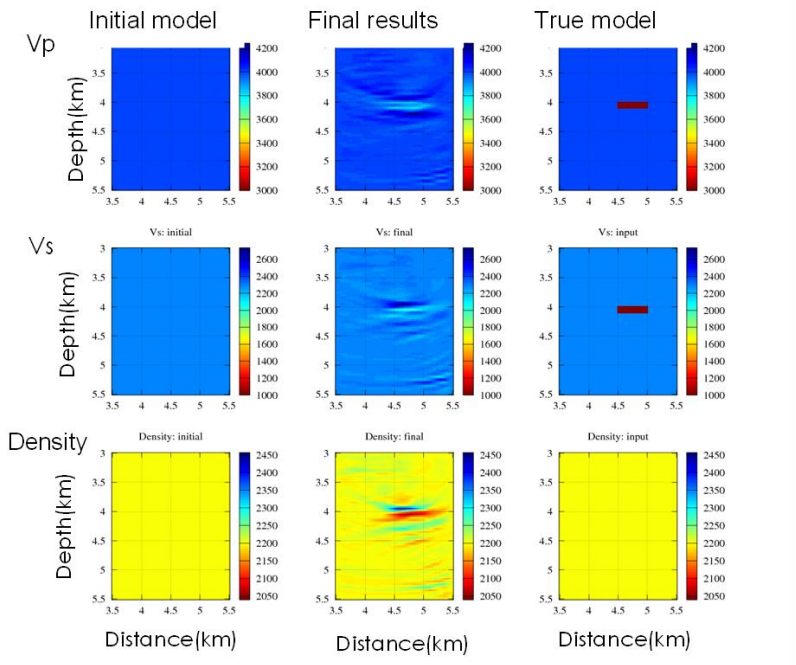

Figure 7: Result of the first stage of FWI model-2 shown at the center. The true model is shown at the right. The initial model is shown at the left. No density change is assumed.

We apply two stages for the inversion. The first stage mainly focuses on the location and shape. Figure 7 shows the result of the first stage. The location of the assumed reservoir appears to be well retrieved. Using the results of the sensitivity kernels in the first stage, we create the second-stage model, as shown in Figure 8. The final result of FWI model-2 is shown in Figure 9.

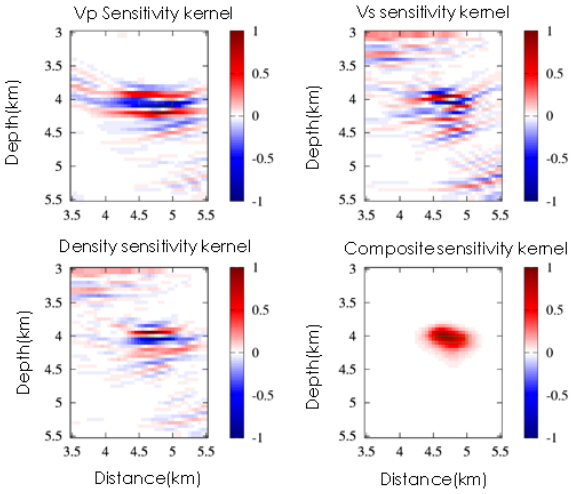

Figure 8: Sensitivity kernels at the first stage of FWI model-2. By combining the three sensitivity kernels, we develop the location and shape of the second stage, as shown at the bottom (right).

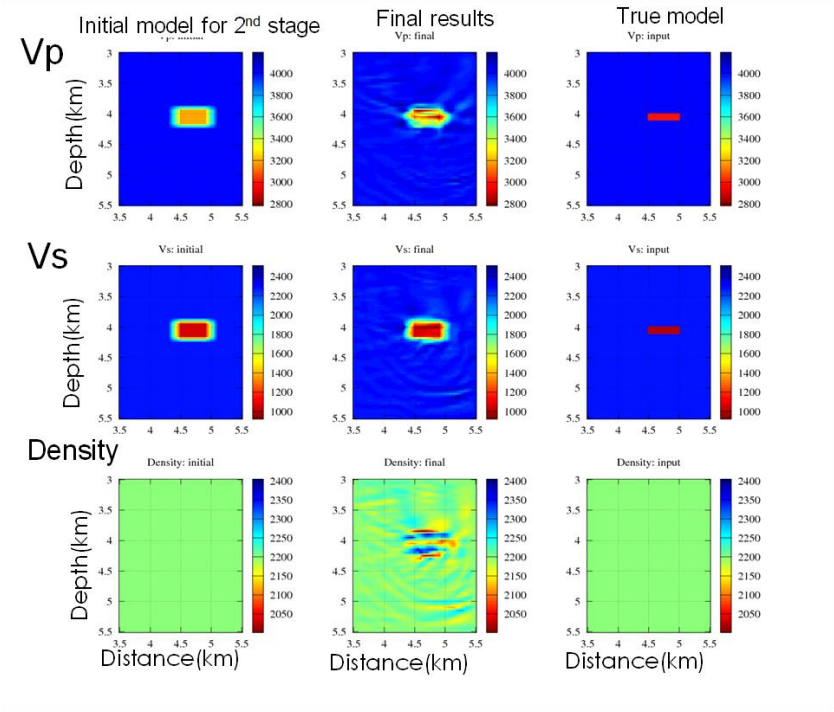

Figure 9: Result of the final results of FWI model-2 shown in the center. The true model is shown in the right column. The initial model of the second stage is shown at the left.

3. 3 Results of the natural earthquakes used as seismic sources (FWI model-3)

We investigate the usefulness of natural earthquakes for imaging of reservoirs. An igneous intrusion is assumed, as shown in Figure 3. Nine natural earthquakes are used as passive seismic sources. Because some natural earthquake activities have been identified just beneath the Medipolis geothermal field, which was the site of the feasibility study, we investigate this case. Unfortunately, however, appropriate seismic activity did not occur during the 2018 feasibility study in the southern Kyushu geothermal field.

The result of FWI model-3 is shown in Figure 10. The retrieved Vp values of the igneous intrusion are concentrated in the intrusion, but a strong smearing zone is identified. Vs in the igneous intrusion is imaged only at the top of the intrusion, and the inside part of the intrusion is not imaged. The density imaging result is similar to the Vp result. By considering the results of this simulation,

imaging that uses natural earthquakes appears to be more difficult than the case that uses active sources although the energy imparted by earthquakes is much larger than that by the active sources.

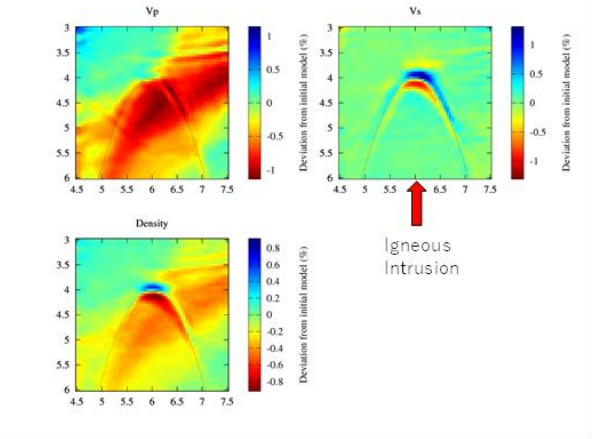

Figure10: Simulation result of the natural earthquakes in FWI model-3 shown in Figure 3. Top left: Vp. Top right: Vs. Bottom: density.

4. DISCUSSION AND CONCLUSIONS

To examine the possibility of imaging supercritical water reservoirs, we carried out three FWI simulations. In FWI model-1, we assumed a borehole seismic source at a depth of 2 km and used the combination of seismic arrays at the surface and in the borehole, observation well, and horizontal well. DAS was used as the array sensor in the borehole, which provided extremely dense seismic data. The result of FWI model-1 showed adequate retrieval of the precise location, shape, and physical properties (Vp, Vs, and density) of the reservoir in the model. However, the contribution of each receiver was not fully investigated.

Considering an actual test situation such as that in the Medipolis geothermal field, we could not use a horizontal well and/or two vertical wells. FWI model-2 reflected more realistic field conditions similar to those in Medipolis. The results of FWI model-2 demonstrated reasonable location and shape of the assumed reservoir, but the assumed physical properties were not well retrieved. The Vp values were better than the Vs values. The reason for the poor retrieval of the physical properties could be probably attributed to the limited aperture of the observed system. Further studies of the receiver and source locations are necessary.

The result of FWI model-3 was less effective than that of FWI model-1. Because we cannot choose the locations and sizes of earthquakes, the use of natural earthquakes for imaging is a bit difficult. However, if we can employ sufficient natural earthquakes, the contribution could be large because the energy supplied by earthquakes is large.

This simulation did not include a noise test. However, if we use ACROSS, which was proposed by Kasahara and Hasada (2016), the background noise can be separated from the source signal using the spectral-comb method. In addition, stacking of data for long duration drastically enhances the S/N. We could use several weeks of data for imaging. Practically, more quantitative evaluation will be needed in the future.

In an actual situation, many factors control the imaging results. One of these factors is the distribution of the supercritical zone. A low-velocity zone might cause scattering of seismic waves. Geology and fractures also strongly affect the imaging.

In conclusion, we believe that the shape and location of supercritical water zones can be identified using the FWI method, seismic observation using active and/or appropriate passive seismic sources, and optical-fiber DAS seismic array. However, retrieval of the physical properties of reservoir(s) can be affected by the aperture of a seismic observation array.

ACKNOWLEDGEMENTS

This presentation is based on the results obtained from a project commissioned by the New Energy and Industrial Technology Development Organization (NEDO). We express our sincere thanks to NEDO and its officers.

REFERENCES

Alkalifah, T. A.: Full waveform inversion in an anisotropic world, Revised edition, EAGE 197pp. (2018)

Bertani, R., Büsing H., Busk S., Dini A., Hjelstuen M., Luchini, M., Manzella A., Nybo R., Rabbe W., Serniotti, L. and the DESCRAMBLE Science and Technology Team: The first results of the DESCRAMBLE project, PROCEEDINGS, 43rd Workshop on Geothermal Reservoir Engineering Stanford University, Stanford, California, February 12-14, 2018 SGP-TR-213 (2018).

Dobson, P., Asanuma, H., Huenges, E., Pletto, F., Reinsch, T., and Sanjuan, B.: Supercritical geothermal system-A review of past studies and ongoing research activities, *Proceedings,* 42th Workshop on Geothermal Reservoir Engineering, Stanford University, Stanford, CA (2017).

Friðleifsson, G. O. , Elders, W.A., Zierenberg, R.A., Stefánsson, A. , Fowler, A.P.G.,Weisenberger, T.B., Harðarson, B.S., and Mesfin, K.G.: The Iceland Deep Drilling Project 4.5 km deep well, IDDP-2, in the seawater-recharged Reykjanes geothermal

field in SW Iceland has successfully reached its supercritical target, Sci. Dril., 23, 1–12, 2017 https://doi.org/10.5194/sd-23-1-2017 (2017).

Hartog, A.: An Introduction to Distributed Optical Fibre Sensors, 442pp, CRC press (2017).

Hasada, Y., Kasahara, J., Kawashima, H., Y. Yamauchi, Y, Sugimoto, Y., Yamaguchi, T. and Kubota, K.: Comparison of the records by optical fiber DAS (Distributed Acoustic Sensor) and geophone using natural earthquakes, JPGU 2018 annual meeting abstract (2018).

Kasahara, J. and Hasada, Y.: Time Lapse Approach to Monitoring Oil, Gas, and CO_2 Storage by Seismic Method", Elsevier Pub., 201pp (2016).

Kasahara, J., Yamaguchi, T., Sugimoto, Y., Kawashima, H., Yamauchi Y., Hasada, Y. and Kubota, K.: Evaluation of fiber optic DAS as a dense seismic array for continuous monitoring of civil engineering structures, JPGU 2018 annual meeting abstract (2018a).

Kasahara, J., Takaichi, K., Suzuki, A., Yamaguchi, T., Mikada, H., Kitaoka, S. and Fujise, Y.: Feasibility study of super critical water reservoirs for the next generation of clean and renewable energy sources, JPGU 2018 annual meeting abstract (2018b).

Kasahara, J., Hasada, Y., Kuzume, H., Fujise, Yamaguchi, and Mikada, H.: Seismic Time-lapse Approach to Monitor Temporal Changes in the Supercritical Water Reservoir, PROCEEDINGS, 43rd Workshop on Geothermal Reservoir Engineering, Stanford University, Stanford, California, February 11-13, 2019, SGP-TR-214 (2019a).

Kasahara, J., Hasada, Y., and Kuzume, H.: A possible geothermal source at around 4 km depth estimated by the seismic observation in Ibusuki geothermal area, JPGU 2019 annual meeting abstract, SVC39-03 (2019b).

Muraoka, H., Uchida, T., Sasada, M., Yagi, M., Akaku, K., Sasaki, M., Yasukawa, K., Miyazaki, S., Doi, N., Saito, S., Sato, K. and Tanaka, S.: Deep geothermal resources survey program: Igneous metamorphic and hydrothermal processes in a well encountering 500°C at 3729 m depth, Kakkonda, Japan., Geothermics, 27(5/6), 507-534(1998).

Reinsch, T., Dobson, P., Asanuma, H., Huenges, E., Pletto F. and Sanjuan, B.: Utilizing supercritical geothermal systems: a review of past ventures and ongoing activities, Geothermal Energy, 10175:16 (2017) https://doi.org/10.1186/s40517-017-0075-y (2017).

Schuster, G. T.: Seismic inversion, Investigations in geophysics. No. 20, SEG (2017)

Suzuki, A., Kasahara, J., Takaichi1, K., Yamaguchi, T., Mikada, H., Kitaoka, S., Fujise Y. and Shimizu, H.: Evaluation of heat retrieval of super-critical water reservoirs and Visualization of Data (2018).

Tarantola, A.: Inversion of seismic reflection data in the acoustic approximation, Geophysics, **49**, 1259-1266 (1984).

Tarantola, A.: A strategy for nonlinear inversion of seismic reflection data, Geophysics, **51**(10), 893-1903 (1986).

Tromp, J, Tape, C., and Liu, Q.: Seismic Tomography, Adjoint Methods, Time Reversal and Banana-Doughnut Kernels, *Geophysical Journal International* 160.1 (2005), 195-216.

Virieus, J. and Opeto, S.: An overview of full-waveform inversion in exploration geophysics, Geophysics, **74** , WCC1-WCC26 (2009).